PostDoc Journal
Vol. 2, No. 1, January 2014

Journal of Postdoctoral Research
www.postdocjournal.com

PVT Property Determination at Elevated Temperatures and Pressures by Floating-Piston Technique

Yue Wu[1,*], Leyuan Xu[2,*], Hao Zhang[3]

[1]Department of Chemical and Life Science Engineering, [2]Department of Biomedical Engineering, [3]Department of Mechanical and Nuclear Engineering, Virginia Commonwealth University, Richmond, Virginia 23284 USA

Email: wuy@vcu.edu (Y. Wu), lxu3@vcu.edu (L. Xu)

Abstract

Pressure-volume-temperature (*PVT*) property data at elevated temperatures and pressures play an important role in a variety of chemical processes and provide a fundamental database for the development and examination of thermodynamic models. This article describes a detailed experimental procedure of the floating-piston technique for determining *PVT* properties of pure liquids and polymer solutions in a wide range of temperatures and pressures. Some representative results using this technique are also given in this article, which agree with available literature data with a percent deviation within $\pm$ 0.4%.

Keywords: density, floating-piston, high pressure, *PVT*

Introduction

Pressure-volume-temperature (*PVT*) properties, also named as densities or volumetric properties, play an important role in the design and optimization of various chemical processes, such as distillation and extraction in the production and purification of oils, polymers, pharmaceuticals, and other natural materials. In many instances, hydrostatic pressure, along with elevated temperature, is applied to make the processes feasible and/or easier. Therefore, high-pressure densities are important fundamental data needed by industry for various practical processes. Density data are also critical fundamental data for the determination of other properties. For example, Density data at elevated pressures are required for the determination and prediction of high-pressure viscosity [1,2], which is another critical property needed in many various chemical processes. In modeling studies, density data at extreme pressures provide a database for testing the performance of contemporary equation of state (EoS) and for improving or establishing a specific EoS suitable for use at high temperatures and pressures [3-10]. The established EoS can then be used to predict important properties such as specific heat, enthalpy, and miscibility [11-14].

High-pressure fluid densities are mostly measured using one of three techniques, including vibrating-body, bellows, and floating-piston method. A general review of the principles, strengths, and weakness of the techniques is given in detail elsewhere [15]. Among these techniques, the floating-piston technique has been used to determine densities at extreme temperatures if the o-rings are carefully chosen [16]. Unlike vibrating-body and bellows techniques, the floating-piston technique also allows for the observation of the fluid of interest. Hence, it is possible to simultaneously determine the density and phase behavior with the same apparatus [17].

This article will give a detailed description of the methodology for the high-temperature, high-pressure density determination. A typical floating-piston apparatus will be introduced, and then the experimental procedures will be given in detail for the density determination. Last, some representative results will be presented.

Apparatus

A typical example of the experimental floating-piston system is illustrated in Figure 1, which consists of a high-pressure view cell, linear variable differential transformer (LVDT), pressure transducer, temperature control and measurement system, display system, and thermoset insulation [17]. The schematic diagram of the view cell and LVDT is shown in Figure 2 [7]. A cylindrical view cell, constructed of high nickel content steel (Nitronic 50TM), is 7.00 cm outside diameter, 1.59 cm inside diameter, and approximately 35 ml working volume. A 1.9 cm outside diameter by 1.9 cm thick sapphire window is fitted into one end of the cell. The window is sealed by a 116 viton o-ring (15/16" O.D., 3/4" I.D.) and a 116 EPR backup o-ring. After securing the window in the cell, the end cap is bolted to the cell body. The cell is flipped vertically, and a stir bar is loaded in the cell followed by the piston. For the piston, a 205 viton o-ring (11/16" O.D., 7/16" I.D.) is used to separate the cell contents from water, which is the hydraulic fluid used to move the piston. Then a rod with a magnetic end piece, called a core, is connected to the piston so that the rod extends out of the cell. The core travels through an LVDT (Schaevitz Corp., Model 2000 HR) that senses the position of core. A type-K thermocouple (Omega Corporation) connected to one of the side ports is used to measure the temperature of the fluid in the view cell, which is housed in an air bath. The cell is also wrapped with heating bands to obtain very high operating temperatures. The typical control of the temperature of the heating bands is ± 0.2 K. After loading the fluid of interest into the cell through a side port, the water is pressurized by the high-pressure generator (HIP Inc., model 37-5.75-60), pushing the piston forward to compress the fluid of interest. The system pressure is measured by a calibrated pressure transducer (Viatran Corporation, Model 245, 0 - 50,000 psig (345 MPa), accurate to ± 50 psig (0.35 MPa)) on the water side of the piston.

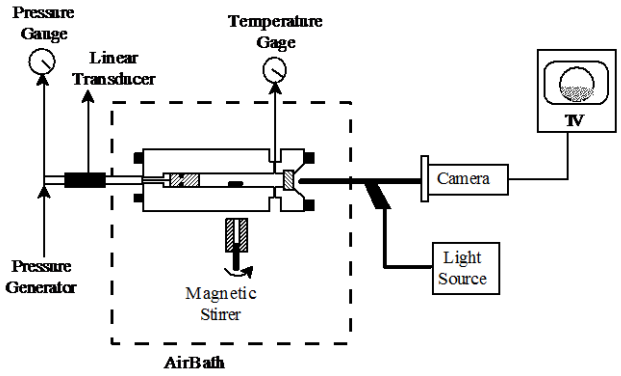

Figure 1. Schematic diagram of the experimental system used in this study to obtain high-pressure density measurements. Reproduced from reference [17].

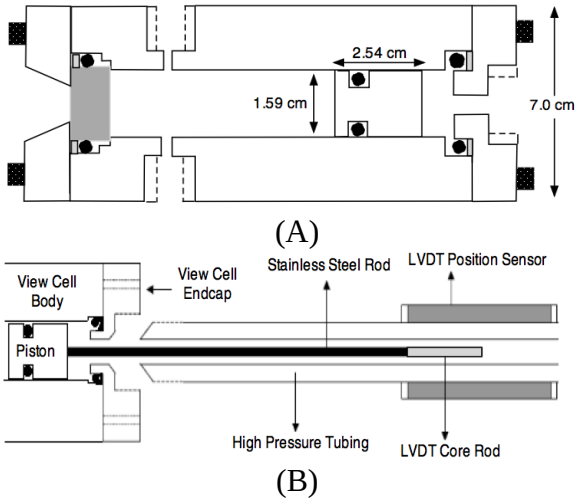

Figure 2. Schematic diagram of (A) the high-pressure view cell used in this study, and (B) the LVDT used for volume measurements. Reproduced from reference [7].

Experimental Procedure

Calibration

The transducer used to determine the pressure in the view cell is calibrated against a Heise pressure gauge (Heise Corporation, Model CC, 0 - 10,000 psig (68.9 MPa)), accurate to ± 10 psig (0.07 MPa) for pressures below 10,000 psig and an identical Viatran-calibrated pressure

transducer (Viatran Corporation, Model 245, 0 - 50,000 psig (345 MPa)), accurate to ± 50 psig (0.35 MPa), is used to measure pressures from 10,000 to 40,000 psig (275 MPa). Since the pressure transducer is on the water side of the piston and will be always used at room temperature during the experiment, the pressure calibration experiments are performed at room temperature. Since the view cell pressure transducer is within ± 10 psig (0.07 MPa) of the Heise gauge when pressure is below 8,200 psig (55.8 MPa), the transducer is considered accurate to ± 10 psig (0.07 MPa) when pressure is below 8,200 psig and ± 50 psig (0.34 MPa) when pressure is from 8,200 to 30,000 psig (206 MPa).

The type-K thermocouple is calibrated against a precision immersion thermometer (Fisher Scientific, 308 to 473 K, precise to 0.1 K, accurate to better than ± 0.10 K, recalibrated by ThermoFisher Scientific Company at four different temperatures using methods traceable to NIST standards) using a temperature-controlled silicone oil bath (Dow Company, Syltherm 800, recommended for 253 K to 473 K) at atmosphere pressure.

The internal cell volume is calibrated against the LVDT reading with pure n-decane (99.0% purity) at 323, 423 and 523 K. Before an experiment, air in cell is removed by flushing three times with a gas at room temperature and a pressure of ~150 psig (1.0 MPa). The structure of the flushing gas is similar to the liquid solvent of interest. A 10 mL syringe is used to load 7.0 to 9.0 ± 0.0001 grams of n-decane through the top port of the cell. The exact mass of the loaded fluid is calculated by subtracting the mass of the syringe and n-decane before loading from the mass of the syringe and fluid after loading, both of which are weighed by a scale accurate to 0.0001 gram. The amount of air that enters the cell is ignored during this process. The temperature is increased and stabilized at around 50°C followed by increasing the pressure in the cell up to 40,000 psig. The LVDT readings are recorded at around 4,000 psig (27 MPa), 8,000 psig (54 MPa), 12,000 psig (82 MPa), 16,000 psig (109 MPa), 20,000 psig (136 MPa), 25,000 psig (170 MPa), 30,000 psig (204 MPa), 35,000 psig (238 MPa) and 40,000 psig (275 MPa). The cell is maintained at each temperature and pressure for around 10 minutes to allow the temperature to stabilize so that the fluctuation of T is less than ± 0.30 K. It should also be noted that the pressure is not increased monotonically, but it is changed randomly from low pressure to high pressure to avoid any systematic error. Therefore, the internal volume of the cell is determined by dividing the mass of the loaded n-decane by the density obtained from the NIST Chemistry Webbook [18] at a given temperature, pressure, and LVDT reading. The calibration is repeated with a new loading of n-decane at 423 K and 523 K to account for any temperature effects on the cell volume. All of the calibration experiments are performed with the stir bar in the cell. The calibration curve for the internal volume can be represented as

$$V_{Cell} = S \cdot T.R. + I \quad (1)$$

where V_{Cell} is the internal cell volume and *T.R.* is the LVDT reading. *S* and *I* are the slope and intercept, respectively. σ_S and σ_I refer to the uncertainties of slope and intercept of the internal cell volume calibration curve, respectively.

3.2. Density Determination

The experimental procedure for measuring densities is similar to the technique used to calibrate the cell: flush the cell three times to remove the air inside it, load 7.0 to 9.0 ± 0.0001 grams of the testing fluid, increase the pressure in stages to 40,000 psig (275 MPa), and record the LVDT reading at each *P* and *T*. Since the relationship between the internal cell volume and the LVDT reading has been set by the previous calibration step, the density of the fluid loaded into the cell can be obtained by dividing the mass of the fluid by the cell internal volume at a given *P* and *T*. All the density measurements

are taken with the stir bar in the cell and each density data point is obtained by randomly changing the system pressure instead of always increasing from low pressure to high pressure to avoid any potential systematic error. The cell is maintained at a given *P* and *T* for 10 minutes to ensure that the temperature variation is less than ± 0.2 K. Figure 3 shows the temperature fluctuation with time after increasing the pressure from atmosphere pressure to 4,000 psig (27 MPa) at around 423 K for n-pentane [19]. These data show that 10 minutes is long enough for the stabilization of the temperature. Although waiting for a longer time is better for reducing the level of temperature fluctuation, operating at high temperatures for a long period of time may lead to the degradation of the o-rings.

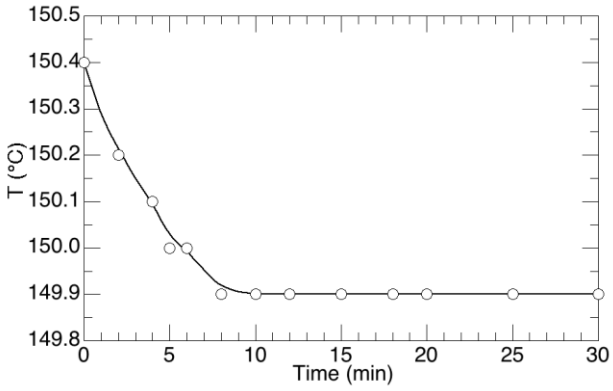

Figure 3. Variation of the cell internal temperature after increasing the pressure from atmospheric pressure to 4,000 psig (28 MPa) at around 423 K. Reproduced from reference [19].

Error Analysis

The standard uncertainties of pressures and temperatures are σ_T = 0.20 K and σ_P = 0.07 MPa. Given that the density, ρ, equals to the mass, m, divided by the volume, V, the experimental uncertainty of densities can be estimated by the summation of each partial derivatives of each variable shown in Equation 2,

$$\sigma_\rho = \sqrt{\left(\frac{\partial \rho}{\partial m}\right)^2 \sigma_m^2 + \left(\frac{\partial \rho}{\partial V}\right)^2 \sigma_V^2} = \sqrt{\left(\frac{1}{V}\right)^2 \sigma_m^2 + \left(\frac{m}{V^2}\right)^2 \sigma_V^2} \quad (2)$$

where σ_ρ, σ_m, and σ_V are the uncertainties of density, mass, and volume, respectively. σ_m can be obtained directly from the weighing scale, which is 0.0001. σ_V can be calculated based on the aforementioned internal calibration equation of internal cell volume against the LVDT reading, *T.R.* by using the partial derivative equations, given as

$$\sigma_V = \sqrt{\left(\frac{\partial V}{\partial I}\right)^2 \sigma_I^2 + \left(\frac{\partial V}{\partial S}\right)^2 \sigma_S^2 + \left(\frac{\partial V}{\partial T.R.}\right)^2 \sigma_{T.R.}^2} = \sqrt{\sigma_I^2 + T.R.^2 \sigma_S^2 + S^2 \sigma_{T.R.}^2} \quad (3)$$

where *I* is the intercept and *S* is the slope of the volume calibration equation. Correspondingly, σ_I, σ_S, and $\sigma_{T.R.}$ are the uncertainties of intercept, slope, and LVDT reading. σ_I and σ_S can be calculated from the linear fitting of *V* against *T.R.*, which are 0.0345 and 0.0004, respectively. $\sigma_{T.R.}$ can be directly obtained from the company specification of the LVDT used in this study, which is 0.0025. Therefore, the estimated accumulated experimental uncertainty is σ_ρ = 0.75% × ρ.

Representative Results

Figures 3 through 5 show the density data for o-xylene, m-xylene, and p-xylene obtained in this study at pressures to 265 MPa and temperatures to 525 K [9]. Note that a liquid-solid phase boundary is crossed for o-xylene and p-xylene, termed as “solid” in the figures. Details are found elsewhere on the high-pressure solidification behavior for these aromatic hydrocarbons [17].

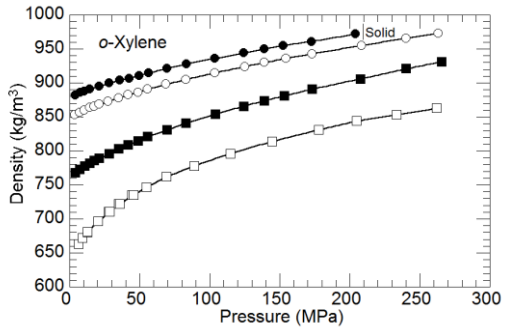

Figure 4. Density data for o-xylene at the temperatures of 294.9 K (●), 325.0 K (○), 423.9 K (■), and 523.2 K (□). Solid lines are used to guide the eyes. Reproduced from reference [9].

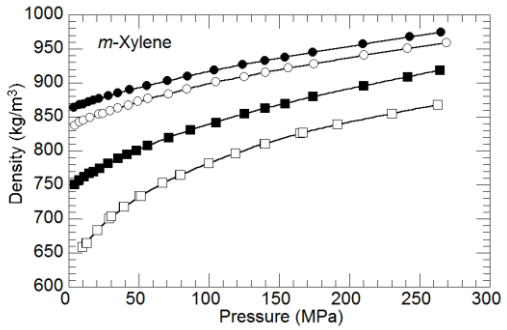

Figure 5. Density data for m-xylene at the temperatures of 295.7 K (●), 325.4 K (○), 422.4 K (■), and 522.9 K (□). Solid lines are used to guide the eyes. Reproduced from reference [9].

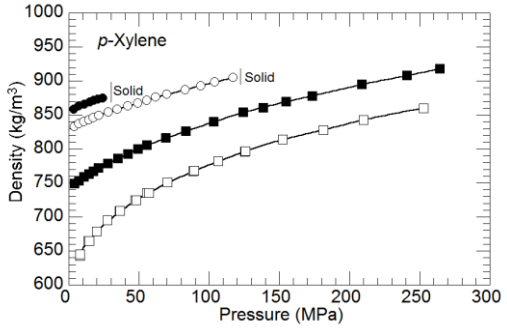

Figure 6. Density data for p-xylene at the temperatures of 295.0 K (●), 325.7 K (○), 423.3 K (■), and 523.0 K (□). Solid lines are used to guide the eyes. Reproduced from reference [9].

Figures 6 through 8 show the percent deviation between available literature data and the experimental densities obtained by the floating-piston technique. Note the maximum temperature in these figures is 370 K except for the case of m-xylene since Caudwell et al. [20] reported m-xylene density data to 473 K. Figures 6 through 8 also do not include density data reported at atmospheric pressure [21-25] or data that cover a very limited pressure range [26-28]. The largest percent deviation is less than 0.40% for all of the aromatics considered in this study, suggesting a good agreement between the experimental data and literature data.

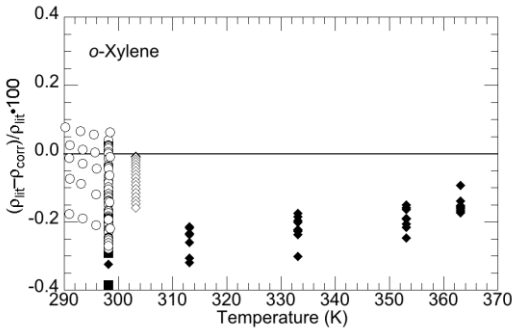

Figure 7. Percent deviation for o-xylene densities between experimental data obtained in this study, $\rho_{i,corr}$, and literature data, $\rho_{i,lit}$, of Bridgman [29] (■), Et-Tahir et al. [30] (♦), Takagi et al. [31] (◊), and Taravillo et al. [32] (○).

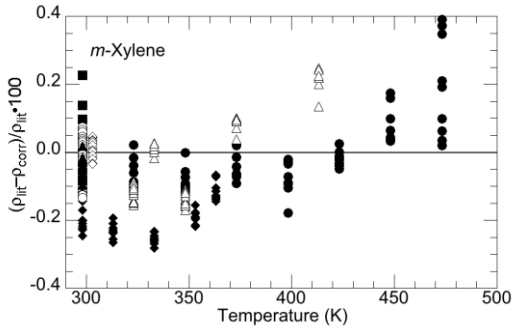

Figure 8. Percent deviation for m-xylene densities between experimental data obtained in this study, $\rho_{i,corr}$, and literature data, $\rho_{i,lit}$, of Bridgman [29] (■), Caudwell et al. [20] (●), Chang et al. [33,34] (Δ), Et-Tahir et al. [30] (♦),

Takagi et al. [35] (◊), Taravillo et al. [36] (○), and Yokoyama et al. [37] (▲).

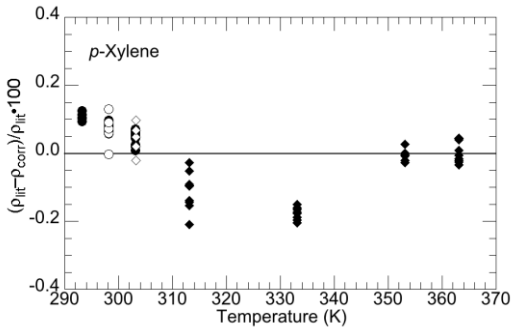

Figure 9. Percent deviation for p-xylene densities between experimental data obtained in this study, $\rho_{i,corr}$, and literature data, $\rho_{i,lit}$, of Castro et al. [38] (●), Et-Tahir et al. [30] (♦), Takagi et al. [35] (◊), and Yokoyama et al. [37] (○).

Conclusion

This article describes in detail the experimental procedures for determining high-pressure densities with the floating piston technique. The estimated accumulated uncertainty of experimental density data is within ± 0.75%. The experimental densities are compared with available literature data for three xylene isomers, which only cover densities at limited temperatures and pressures. The experimental density data using the floating-piston technique agree with the literature data within ± 0.4%. The deviation between experimental data and literature data is lower than the estimated accumulated uncertainty of experimental densities, showing a good accuracy for using the experimental floating-piston technique.

Acknowledgements

This technical effort was performed in support of the National Energy Technology Laboratory's Office of Research and Development support of the Strategic Center for Natural Gas and Oil under RES contract DE-FE0004000.

Reference

[1] H. Baled, D. Tapriyal, B. Morreale, Y. Soong, I. Gamwo, V. Krukonis, B. Bamgbade, Y. Wu, M. McHugh, W. Burgess, R. Enick, Int J Thermophys (2013) 1-20.

[2] W.A. Burgess, D. Tapriyal, B.D. Morreale, Y. Soong, H.O. Baled, R.M. Enick, Y. Wu, B.A. Bamgbade, M.A. McHugh, Fluid Phase Equilib. 359 (2013) 38-44.

[3] H. Baled, R.M. Enick, Y. Wu, M.A. McHugh, W. Burgess, D. Tapriyal, B.D. Morreale, Fluid Phase Equilib. 317 (2012) 65-76.

[4] B.A. Bamgbade, Y. Wu, H.O. Baled, R.M. Enick, W.A. Burgess, D. Tapriyal, M.A. McHugh, J. Chem. Thermodyn. 63 (2013) 102-107.

[5] B.A. Bamgbade, Y. Wu, W.A. Burgess, M.A. McHugh, Fluid Phase Equilib. 332 (2012) 159-164.

[6] W.A. Burgess, D. Tapriyal, B.D. Morreale, Y. Wu, M.A. McHugh, H. Baled, R.M. Enick, Fluid Phase Equilib. 319 (2012) 55-66.

[7] K. Liu, Y. Wu, M.A. McHugh, H. Baled, R.M. Enick, B.D. Morreale, J. of Supercrit. Fluids 55 (2010) 701-711.

[8] Y. Wu, B. Bamgbade, K. Liu, M.A. McHugh, H. Baled, R.M. Enick, W.A. Burgess, D. Tapriyal, B.D. Morreale, Fluid Phase Equilib. 311 (2011) 17-24.

[9] Y. Wu, B.A. Bamgbade, H. Baled, R.M. Enick, W.A. Burgess, D. Tapriyal, M.A. McHugh, Ind. Eng. Chem. Res. 52 (2013) 11732-11740.

[10] Y. Wu, B.A. Bamgbade, W.A. Burgess, D. Tapriyal, H.O. Baled, R.M. Enick, M.A. McHugh, J. Phys. Chem. B 117 (2013) 8821-8830.

[11] S. Dabiri, G. Wu, M.T. Timko, A.F. Ghoniem, J. of Supercrit. Fluids 67 (2012) 29-40.

[12] G. Wu, S. Dabiri, M.T. Timko, A.F. Ghoniem, J. of Supercrit. Fluids 72 (2012) 150-160.

[13] G. Wu, S. Dabiri, M.T. Timko, A.F. Ghoniem, Mixing of hydrocarbon droplets and water at supercritical or near-critical conditions. 10th International Symposium on Supercritical Fluids, San Francisco, CA, USA, 2012.

[14] G. Wu, Journal of Postdoctoral Research 1 (2013) 26-28.
[15] Y. Wu, L. Xu, H. Zhang, X. Zeng, J. Chen, Journal of Postdoctoral Research 1 (2013) 22-31.
[16] E.U. Franck, S. Kerschbaum, G. Wiegand, Ber. Bunsen-Ges. Phys. Chem. Chem. Phys. 102 (1998) 1794-1797.
[17] Y. Wu, K. Liu, B.A. Bamgbade, M.A. McHugh, Fuel 111 (2013) 75-80.
[18] E.W. Lemmon, M.O. McLinden, D.G. Friend, "Thermophysical Properties of Fluid Systems" in **NIST Chemistry WebBook, NIST Standard Reference Database Number 69**, Eds., P.J. Linstrom, W.G. Mallard, National Institute of Standards and Technology, Gaithersburg MD, 20899, http://webbook.nist.gov, (retrieved December 16, 2012).
[19] Y. Wu, High-pressure and high-temperature density measurements of n-pentane, n-octane, 2,2,4-trimethylpentane, cyclooctane, n-decane, and toluene. Master Thesis, Viriginia Commonwealth University, 2010.
[20] D.R. Caudwell, J.P.M. Trusler, V. Vesovic, W.A. Wakeham, J. Chem. Eng. Data 54 (2009) 359-366.
[21] J.L. Hales, R. Townsend, J. Chem. Thermodyn. 4 (1972) 763-772.
[22] J.M. Geist, M.R. Cannon, Ind. Eng. Chem., Anal. Ed. 18 (1946) 611-613.
[23] S.C. Bhatia, R. Rani, R. Bhatia, J. Chem. Eng. Data 56 (2011) 1675-1681.
[24] Y.-Y. Yang, Y.-M. Zhu, J.-L. Peng, J.-C. Chen, P.-P. Feng, Z.-Q. Huang, J. Chem. Thermodyn. 41 (2009) 1000-1006.
[25] H. Zarei, Z. Salami, J. Chem. Eng. Data 57 (2012) 620-625.
[26] S.K. Garg, T.S. Banipal, J.C. Ahluwalia, J. Chem. Thermodyn. 25 (1993) 57-62.
[27] Z. Fang, Y. Qiao, Z. Di, Y. Huo, P. Ma, S. Xia, J. Chem. Eng. Data 53 (2008) 2787-2792.
[28] T. Yang, S. Xia, Z. Di, P. Ma, Chin. J. Chem. Eng. 16 (2008) 247-255.
[29] P.W. Bridgman, Proc. Am. Acad. Arts Sci. 77 (1949) 129-146.
[30] A. Et-Tahir, C. Boned, B. Lagourette, P. Xans, Int J Thermophys 16 (1995) 1309-1334.
[31] T. Takagi, H. Teranishi, J. Chem. Thermodyn. 17 (1985) 1057-1062.
[32] M. Taravillo, S. Castro, V.G. Baonza, M. Caceres, J. Nunez, J. Chem. Soc.-Faraday Trans. 90 (1994) 3527-3532.
[33] J.S. Chang, M.J. Lee, J. Chem. Eng. Data 40 (1995) 1115-1118.
[34] J.S. Chang, M.J. Lee, H.M. Lin, J. Chem. Eng. Data 41 (1996) 1117-1120.
[35] T. Takagi, J. Chem. Thermodyn. 13 (1981) 291-299.
[36] M. Taravillo, S. Castro, V.G. Baonza, M. Caceres, J. Nunez, J. Chem. Soc.-Faraday Trans. 90 (1994) 1217-1221.
[37] C. Yokoyama, S. Moriya, S. Takahashi, Fluid Phase Equilib. 60 (1990) 295-308.
[38] S. Castro, M. Taravillo, V.G. Baonza, M. Caceres, J. Nunez, J. Chem. Soc., Faraday Trans. 90 (1994) 3645-3649.